Effect of Mooring Line Materials on FKT System Dynamics

Jo-Ti Wu[#1], Jiahn-Horng Chen[#2], Ching-Yeh Hsin[#3], Forng-Chen Chiu[*4]

[#]*Department of Systems Engineering and Naval Architecture, National Taiwan Ocean University*
2 Pei-Ning Road, Keelung 202, Taiwan

[1]rortyaa@gmail.com

[2]b0105@mail.ntou.edu.tw

[3]hsin@mail.ntou.edu.tw

[*]*Department of Engineering Science and Ocean Engineering, National Taiwan University*
1 Roosevelt Road Sec. 4, Taipei 104, Taiwan

[4]fcchiu@ntu.edu.tw

***Abstract*— In Taiwan, a floating Kuroshio turbine (FKT) system is under development by the joint research team of National Taiwan University and National Taiwan Ocean University. One of the issues which need be studied is its dynamics moored in deep sea. To understand the effects of mooring line materials on the system dynamics, we studied computationally the dynamic behaviors of the FKT moored with flexible ropes, chains, and 6×19 wire with wire core. In this study, we integrated several commercial and in-house packages. The system buoyancy and weight and their centres were estimated using the Rhino software. The system hydrodynamic coefficients were obtained through WAMIT, system drag coefficient through FLUENT, turbine propulsive force through lifting surface code, and system dynamics through OrcaFlex. We investigated the dynamic responses of the FKT system under waves with single frequency and random waves with different typical spectra.**

***Keywords*— Ocean current energy; floating turbine system; mooring line system; mooring line material; system dynamics**

I. INTRODUCTION

The development of marine energy has become a new frontier of technology research all over the world. Many technological challenges have been addressed. Coping with these challenges, various converters were devised for harnessing different kinds of marine energy in the past several decades. Among them are the ocean current turbine systems which, in fact, represent another level of deep-water technology. With the advancement of technology, several prototypes of ocean energy devices have been developed, e.g. [1-6].

One of the key issues in harnessing ocean current energy is the deep-sea mooring system which connects the current turbine floating in the ocean current and the anchor of some kind on the sea bed. This was a new research topic in the past decade. The interdependency between the mooring and ocean current turbine systems plays a crucial role early in the design phase. Many studies have been conducted. Each of them was mostly limited to some particular kind of ocean current turbine and mooring systems.

Cribbs [7] developed a numerical procedure to model the mooring system for the 20 kW current turbine system proposed by a research team at Center for Ocean Energy Technology of Florida Atlantic University. He attempted to optimize the mooring attachment locations on the floating body, the tether arrangement, and locations of two floating devices attached to the mooring line. Cribbs and VanZwieten [8] also studied in details sensitivity of system responses to parametric variations. Shibata *et al*. [9] conducted both experimental and numerical studies to investigate the stability of a V-shape mooring system connected to an ocean turbine developed by Takagi *et al*. [10]. Rho *et al*. [11] proposed methods to select and optimize the mooring system for tidal turbine system which is located in shallow water regions. They concluded that the SPAR type had better performances for a multi-arrayed system. More recently, Tsao and Feng [12] have developed the cross-stream active mooring system to adjust the horizontal position of a current turbine in order to tract fast streams to increase power generation capacity.

Wave is a source of system instability for a moored ocean current turbine system. Their interaction is an important issue in developing the floating current turbine systems. Shirasawa *et al*. [13] tested the system dynamics of the ocean current turbine with a single mooring line under the action of waves. Though the ocean current turbine works at the middle layer of a water flow, the influence is significant. They pointed out that when the wave length was long, compared to the turbine operation depth, the mooring method was important to make the deployment stable. Wu *et al*. [14] investigated the effects of mooring line design and waves on dynamics of the current turbine system developed by the research team of National Taiwan University and National Taiwan Ocean University. Their results show that the surface waves induce system pitching oscillation which becomes significant when the wave propagation is parallel to the current flow and its period is close to the system resonant periods.

Recently, Cribbs *et al*. [15] have surveyed the existing mooring standards. They pointed out that modelling mooring dynamics could be complicated and the loads and fatigue cycles of a mooring system easily underestimated due to unexpected marine environments. It implies that more studies are indispensable to understand fully the interaction between the

mooring and current turbine systems in very dynamic ocean environments. Finally, it is worth mentioned that some studies were also conducted for mooring systems applied to tidal stream current turbines. Bowie [16] argued that flexible mooring system offered advantages for tidal current turbines in installation and maintenance. Jo *et al*. [17] also investigated the mooring system with a duct-type tidal current turbine system in shallow water.

II. The Floating Kuroshio Turbine System

The floating Kuroshio Turbine (FKT) is a system composed of five major components, as shown in Fig. 1. The floating-foil is equipped with four buoyancy engines. These engines can be used for flooding or drainage in order to adjust the gravity centre of the system, the buoyancy, and the attitude of the foil which produces dynamic lift. Two vertical supports connect the foil float and the ocean current turbine generator system. The cross beam connects the twin turbines. The two rotors harness the kinetic energy of ocean current and transform it into electricity by the generators inside the nacelles. To maintain proper stability during deployment, operation, and recovery, the concept of the downwind turbine system is adopted.

In the present study, the 1/5 model was adopted. For this model, the chord length and span are 4.0 m and 7.5 m, respectively and the rated power is 20kW when the current speed is 1.5m/sec. The water depth is assumed to be 50 m. The design operation depth for the model FKT system is 10-40m. A single-line mooring system is provided. It consists of two short auxiliary lines and one main line to form a Y-shape system. The two auxiliary lines are connected to the foremost points of nacelles to the incoming current and join together with a connector to the main line which is then connected to the anchor on the bottom. We assume that the end of each line can freely slide on the connector. The length of the main line is 40 m long and each of the auxiliary lines connecting the turbine system and the main line is 5m long.

III. Approach of Study

The study was conducted computationally. The force system acting on the FKT system is complicated, including buoyancy, weight, drag due to the current passing the system and the mooring lines, dynamic lift due to the floating-foil, tension force exerted by the mooring line, and the propulsive force produced by the rotation of the contra-rotating turbines. Furthermore, we also need to consider the effect of added mass.

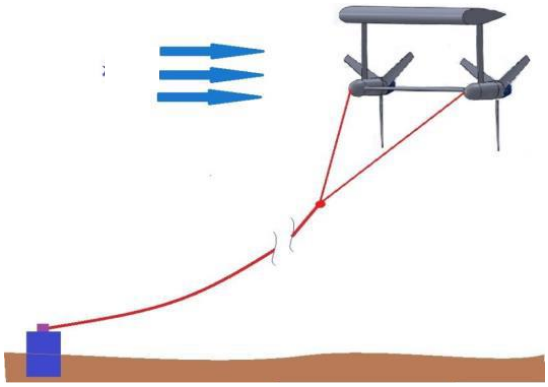

Fig. 1 Schematic of the FKT system with the mooring and anchoring system.

The system buoyancy and weight are directly related to the system design and known from the design data. The buoyancy comes from the weight of water displaced by the system. The design of the turbine blades was conducted computationally by lifting line theory and lifting surface theory. An in-house code has been developed for computations. The floating-foil of finite span provides most of the buoyancy and dynamic lift. The lift coefficient was taken from [18] with the aspect ratio $AR = 2$.

The system resistance was obtained by CFD method. The commercial software FLUENT was employed. The package employs the finite-volume method for discretization. The Reynolds-averaged Navier-Stokes equations were solved with standard k-ε turbulence model. The standard wall function was adopted for flow near the solid wall to handle the low- Reynolds-number flow near the walls. For nonlinear iterations, the SIMPLE algorithm was used. At the condition of uniform incoming flow with a speed of 1.5 m/sec, the resistance was computed and expressed in terms of non-dimensional drag coefficient

$$C_d = \frac{D}{\frac{1}{2}\rho U^2 A} \tag{1}$$

where D is the drag, ρ is the fluid density, U is the uniform incoming current speed, and A is the projected area of the system in the flow direction. According to Lo [19], we have

$$(C_d)_x = 0.173,\ (C_d)_y = 1.184,\ (C_d)_z = 1.318 \tag{2}$$

For the drag coefficients due to circumferential flows, we define

$$(C_d)_M = \frac{M}{\frac{1}{2}\rho\omega^2 A_M} \tag{3}$$

where M is the drag, ω is the angular velocity, and A_M is the area moment of inertia corresponding to the axis about which the outer flow rotate. According to Lo [19], we have

$$(C_d)_{x\text{-axis}} = 0.364,\ (C_d)_{y\text{-axis}} = 0.228,\ (C_d)_{z\text{-axis}} = 0.012 \tag{4}$$

The hydrodynamic coefficients were obtained via another commercial software WAMIT. This code uses boundary element method for discretization. We define several coefficients as follows. For linear motion,

$$C_a = \frac{m_a}{\Delta} \tag{5}$$

where m_a is the added mass and Δ is the displacement of the system. For angular motion,

$$C_a = \frac{I_a}{\Delta \times \ell_c^2} \tag{6}$$

where I_a is the added moment of inertia and ℓ_c is the characteristic length corresponding to the rotating axis. The product $\Delta \times \ell_c^2$ represents the hydrodynamic moment of inertia about the centre of gravity. According to Lo [19], we have the following hydrodynamic coefficients due to linear and angular motions, respectively.

$$(C_a)_x = 0.173,\ (C_a)_y = 0.369,\ (C_a)_z = 4.15 \quad (7)$$

$$(C_a)_{x\text{-axis}} = 18.2,\ (C_a)_{y\text{-axis}} = 4.16,\ (C_a)_{z\text{-axis}} = 1.23 \quad (8)$$

Since the FKT system is moored to an anchor on the sea bed, the mooring line can be modelled with a catenary line. With all the forces shown above, we employed the commercial package OrcaFlex to analyse the system dynamics. This package conducts the simulation in the time domain with nonlinear models. It employs the finite element method for mooring line system discretization and lumped mass element for the FKT system for simplifications. For integration in time, we chose the implicit generalized-α method which damps numerical oscillations with high-frequency dissipations.

IV. Deployment Without Waves

In this study, we studied computationally the dynamic behaviors of the FKT moored with flexible ropes, iron chains, and 6×19 wire with wire core.

A. Polyester Ropes

We considered three cases in which the diameters are d = 3 cm, 10 cm, and 30 cm, respectively. All mooring lines are identical in material and neutrally buoyant. In our computations, we assume that the bulk modulus is infinite, the axial stiffness 700 kN, the bending stiffness 120 kN·m^2, the torsional stiffness 80 kN·m^2, and the Poisson ratio 0.5. The mass per unit length is 0.707 kg/m, 7.854 kg/m, and 70.68 kg/m for d = 3 cm, 10 cm, and 30 cm, respectively.

The dynamic responses of the system at d = 3 cm is shown in Fig. 2. No waves are present in this simulation. It is interesting to find that, shown in Figs. 2(a) and (b), the system appears stable during the flooding process. However, when the turbines start to operate, the FKT system suffers serious pitching and rolling motion for which the amplitude is quickly amplified in a short time.

The results for d = 10 cm are shown in Fig. 3. Similar system fluctuating phenomena are found. Here we show the pitching and heaving motions. The pitching motion results in dynamic lift fluctuations of the foil float and induces system heaving motions. Even though the diameter is increased, the temporal fluctuation in amplitude is almost as big as that for d = 3 cm. However, the pitching growth rate is somewhat smaller and it takes a longer time for the pitching motion to develop.

Shown in Fig. 4 are the results for d = 30 cm. Only the heaving motion is shown here because the deployment is fully stable. No pitching and rolling motions were incurred. The diameter of the mooring line has its significant effects on the system dynamics during deployment. Obviously, it should be big enough to make the system stable during the deployment process.

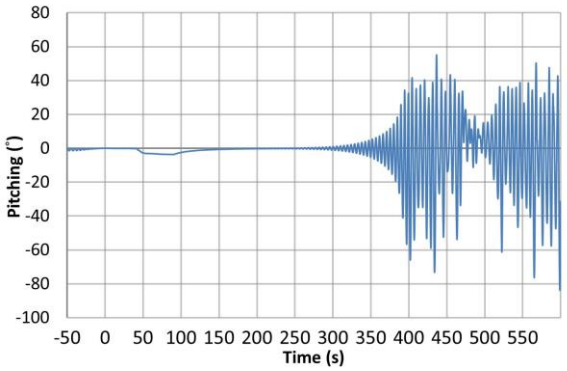

(a) Time-variation of system pitching motion.

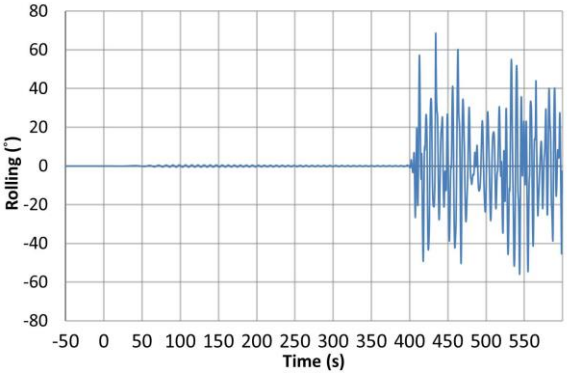

(b) Time-variation of system rolling motion.

Fig. 2 Results for system dynamics with the rope of d = 3 cm.

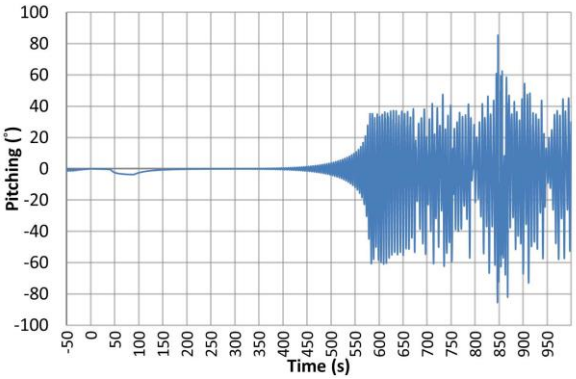

(a) Time-variation of system pitching motion.

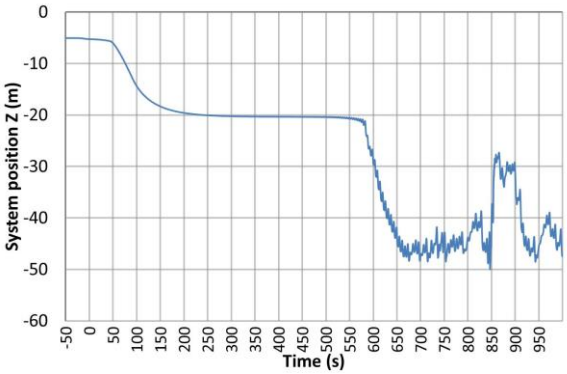

(b) Time-variation of system heaving motion.

Fig. 3 Results for system dynamics with the rope of d = 10 cm.

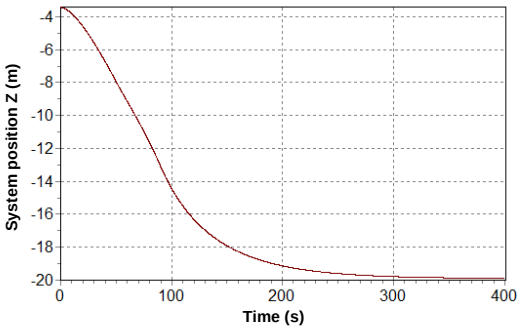

Fig. 4 Time-variation of system heaving motion with the rope of d = 30 cm.

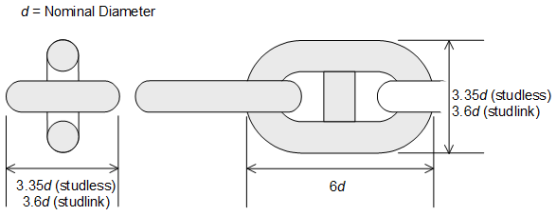

Fig. 5 Geometry of chain used in the present study.

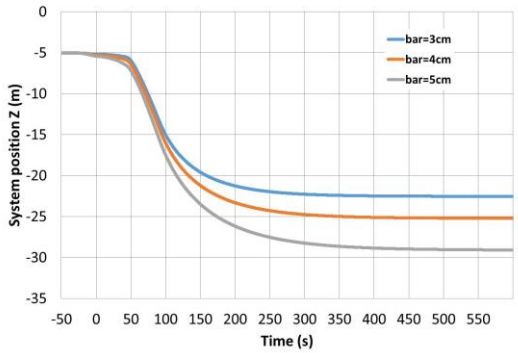

Fig. 6 System heaving motion with iron chains of different diameters.

B. Chains

Shown in Fig. 5 is the geometry of chain employed in the present study. Three different nominal diameters were selected; they are d = 3, 4, and 5 cm. The mass per unit length is $21.9d^2$ te/m, the axial stiffness is $1.01\times10^8 d^2$ kN, and the bending stiffness is 0. The normal and axial drag coefficients are 2.6 and 1.4, respectively. The normal and axial added mass coefficients are 1.0 and 1.4, respectively.

Fig. 6 shows the results of the system heaving motion during the deployment process. For all cases, the motion is stable and the system reaches its final operation position smoothly. Compared to that with flexible ropes, the iron chain can obviously lead to safer and much more satisfactory deployment. Meanwhile, it is also evident that the chain with a larger nominal diameter is heavier per unit length and, therefore, the FKT system sinks to a deeper position at the normal operation condition.

C. 6×19 Wire Rope with Wire Core

Wires have many applications in the offshore industry including towing, mooring and winching. Shown in Fig. 7 is the 6×19 wire rope with wire core which is used in the present study. We assume a value for Young's modulus to be 1.13×10^8 kN/m^2 and axial stiffness $4.04\times10^7 d^2$ kN, respectively. Furthermore, we also assume that the metallic area is 0.455 ($\pi d^2/4$) where d is the nominal diameter of the wire rope as shown in Fig. 7. And the bending stiffness is zero for simplicity. In our investigation, we selected two different values of d which are 3 and 10 cm.

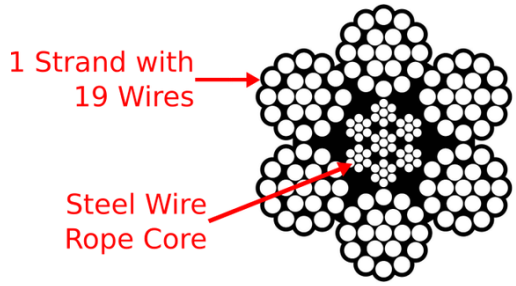

Fig. 7 6×19 wire rope with wire core.

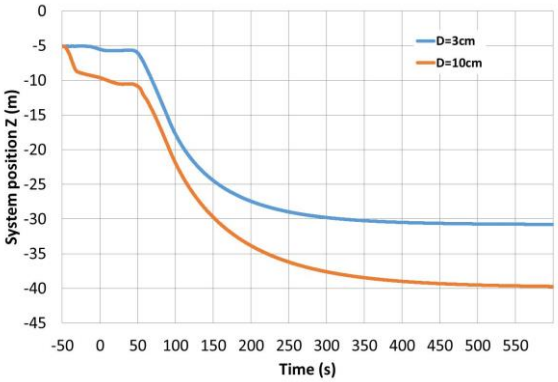

Fig. 8 System heaving motion with wire rope of different diameters.

The results are shown in Fig. 8. They are similar to those shown in Fig. 6. In fact, the wire rope is even heavier. Hence, it can be expected that the deployment would be smooth. Again, there is no system fluctuating motions in all six degrees of freedom. Furthermore, the system operates at an even deeper depth from the free surface when it settles. It is also interesting to note that the deployment takes about the same time duration for the system reaches its stable operating position if the deployment incurs no instability. This can be observed in Figs. 4, 6, and 8.

The study seems to imply that for a smooth deployment, the mooring line should be heavy enough (in terms of its linear mass density). There exists a critical value of the linear mass density for the system to be deployed stably. In fact, we also study the chain in the same shape as that of iron one but of neutral buoyance, the results show that the system deployment is unstable. Therefore, the materials of the mooring line may be of no importance. What matters should be its linear mass density.

V. Deployment With Waves

Now we proceed to the more complicated deployment process with the presence of waves. In fact, this is more practical in a real sea deployment. We assume in the following that the

wave height is 1 m. Since the deployment for the system with flexible ropes is usually not stable in a calm sea if the line diameter is not big enough, we will discuss only the mooring systems with iron chains and wire rope. Moreover, our study also shows that the pitching motion is the most important feature which may result in instability or system fluctuations. Hence, the following discussion will focus on system pitching motion only. Before we proceed to discussion, it should be first mentioned that the system has a natural period of about 5 sec in pitching motion according to Lo [19].

A. Chains

The wave period is a critical parameter which may affect system dynamics. Furthermore, the wave direction is also another parameter which interacts with the system motion. In the following discussion, we assume that the incoming wave is on the opposite direction as that of the current. This could be the most critical wave direction as in Taiwan area, the winter monsoon consistently creates big waves for a few months. The waves also reduce the flow speed of Kuroshio in winter.

If d = 3 cm, the heave motions for different wave periods, T, are shown in Fig. 9. If the period is small, the system reaches its stable operation soon, as shown in Fig. 9(a). Nevertheless, it is obvious that, at T = 5 sec, the system suffers from serious pitching motion. Even at T = 6 sec, the fluctuation in pitching is still significant.

Fig. 10 shows a somewhat different story for d = 4 cm. At T = 4 sec and 6 sec, the long-term behaviours of pitch motion are similar to those when d = 3 cm. However, at T = 5 sec, the pitch fluctuation is much reduced.

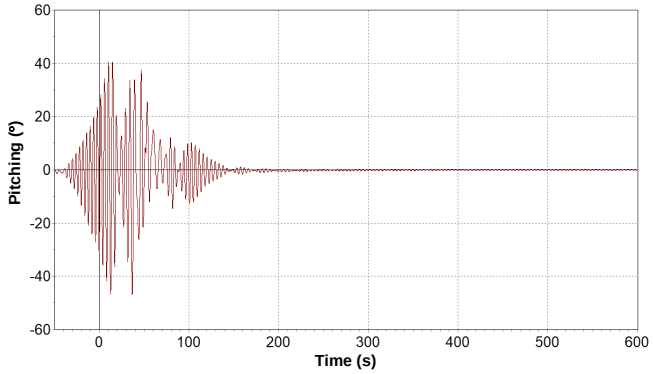

(a) T = 4 sec.

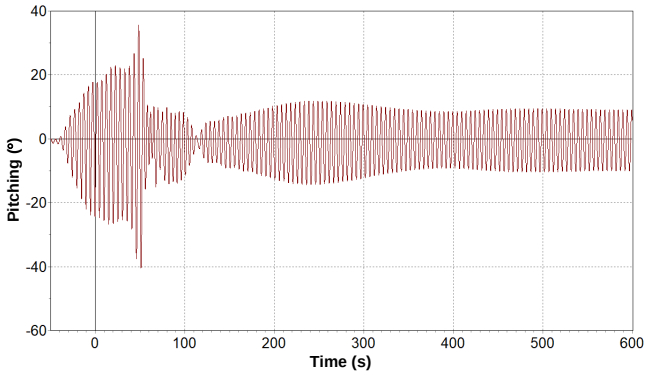

(b) T = 5 sec.

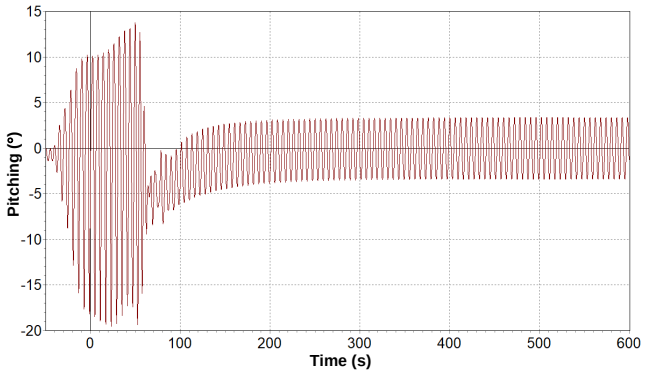

(c) T = 6 sec

Fig. 9 System pitch motion for the iron chain with d = 3 cm.

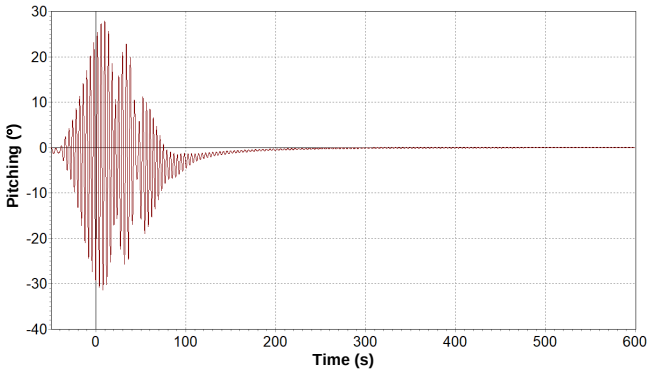

(a) T = 4 sec.

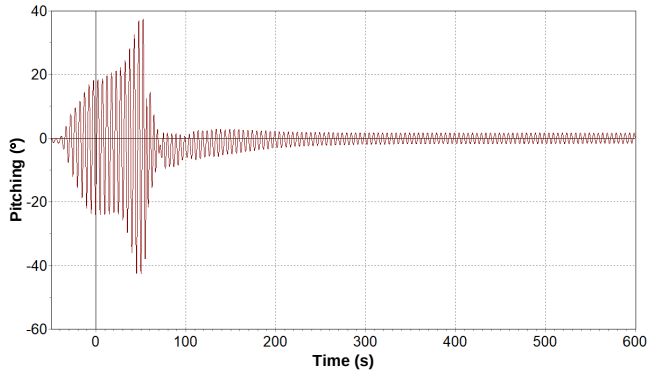

(b) T = 5 sec.

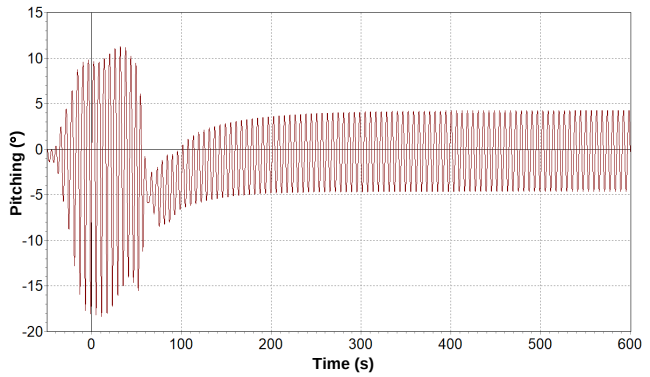

(c) T = 6 sec

Fig. 10 System pitch motion for the iron chain with d = 4 cm.

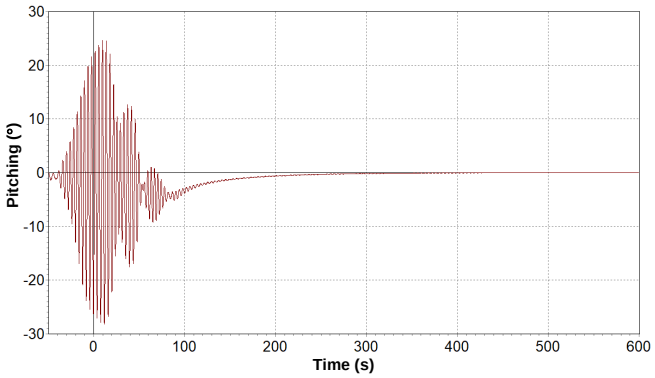

(a) T = 4 sec.

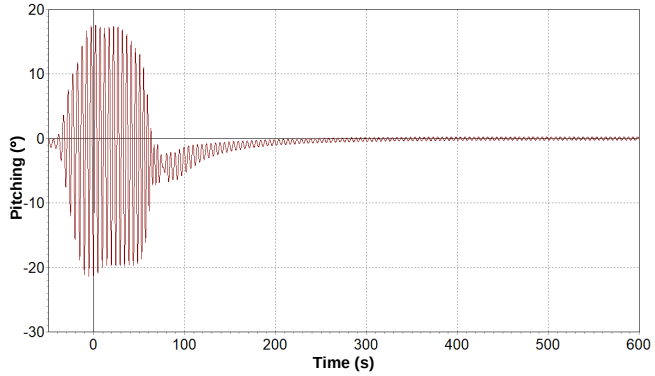

(b) T = 5 sec.

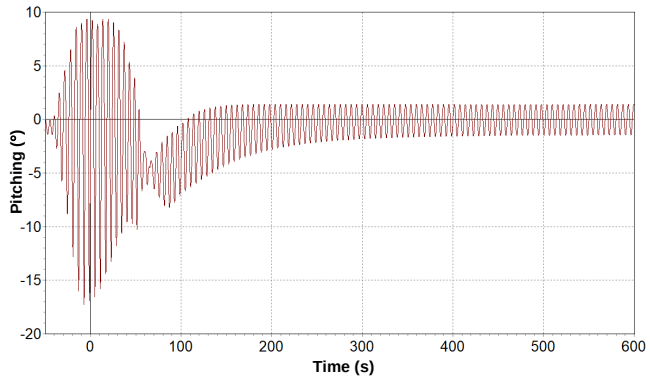

(c) T = 6 sec

Fig. 11 System pitch motion for the iron chain with d = 5 cm.

If d = 5 cm, the results are shown in Fig. 11. The amplitude of fluctuations for all cases are reduced. However, at T = 6 sec, though the pitching is small but still could result in mooring line load fluctuations and fatigue problems in long-term operations.

It should be mentioned that the reduction of pitching fluctuations with a larger chain nominal diameter should be attributed to the fact that the turbine system is located at a deeper position where the water particle motion due to the waves is smaller. Nevertheless, the computational results show evidently that waves have a strong impact on the operation of an ocean current turbine. The influence at least includes the energy harvesting efficiency and system fatigue in long-term operation.

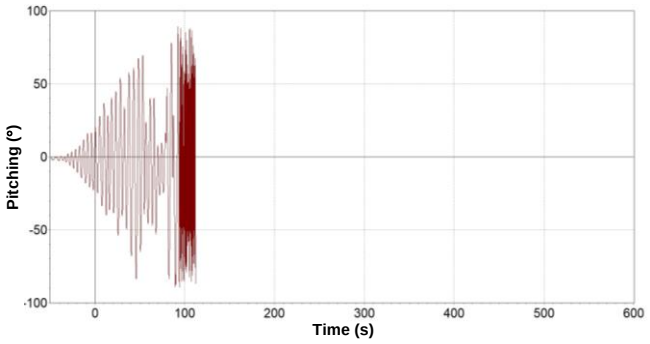

(a) T = 4 sec.

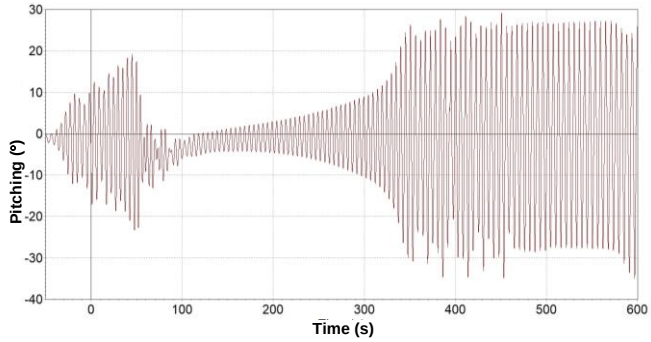

(b) T = 5 sec.

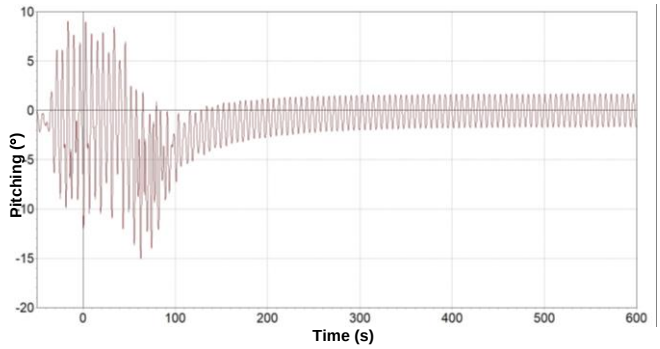

(c) T = 6 sec

Fig. 12 System pitch motion for the wire rope with d = 3 cm.

B. 6×19 Wire Rope with Wire Core

At d = 3 cm, Fig. 12 shows the pitch motion at different wave periods. At T = 4 cm, the computation leads to a blow-up solution which indicates that the system is unstable. At T = 5 sec, the computation does not blow up but the pitch fluctuation is very big and may not be acceptable in practical deployment and operations. The pitching fluctuation is much reduced at T = 6 sec.

Figs. 6 and 8 show that the system with iron chain of d = 5 cm and the one with wire core of d = 3 cm operate at similar depth if no waves are present. However, under the wave action, the system responses shown in Figs. 11 and 12 are not similar. The one with the wire rope is much worse. The mooring with an iron chain appears to exhibit better performance for the present FKT system.

At d = 10 cm, the results shown in Fig. 13 is evidently much improved. The fluctuation of the system pitch motion

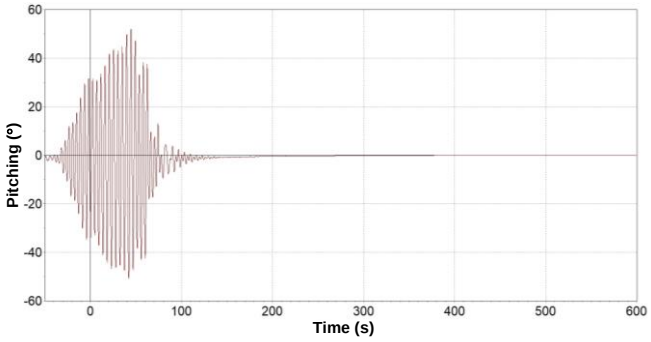

(a) T = 4 sec.

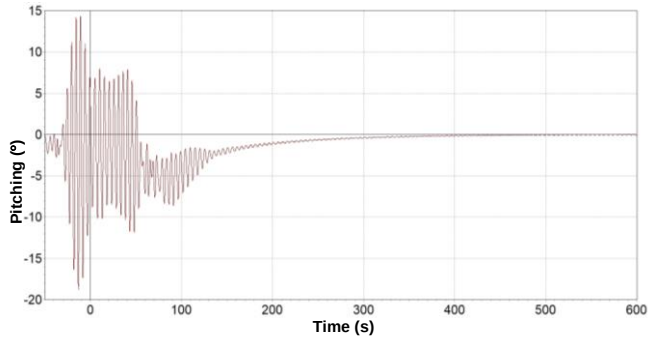

(b) T = 5 sec.

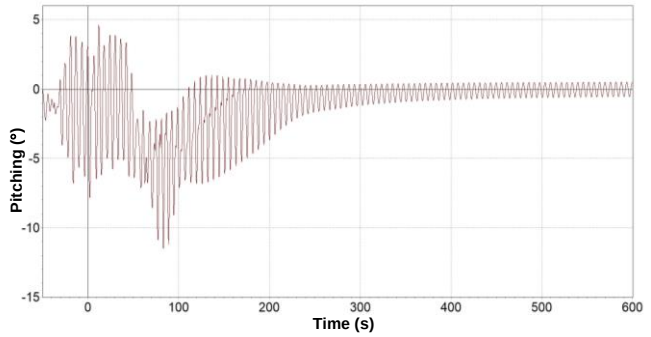

(c) T = 6 sec

Fig. 13 System pitch motion for the wire rope with d = 10 cm.

is greatly reduced. Of course, for this condition, the wire rope is also much heavier, as can be obviously observed in Fig. 8. In fact, the system operates at a depth where is close to the sea bed. The system does not fluctuate at normal operation conditions for T = 4 sec and 5 sec. As to the situation for T = 6 sec, there exists a small amplitude of fluctuation.

Finally, we also investigated the effect of random waves on the system dynamics. Here the results due to two extreme conditions are discussed; the peak periods of the spectrum are T = 9 sec (long wave) and T = 3 sec (short wave), respectively. The spectrum we employed in this study is JONSWAP. The results are shown in Fig. 14. Again, we can find that for the long wave, the system dynamics shows fluctuations in the pitching motion; nevertheless, for the short wave, the system behaves stably. This could be due to the fact that the wave energy is proportional to the wave period. The wave with a longer period possesses more energy which may have stronger influence on the system dynamics.

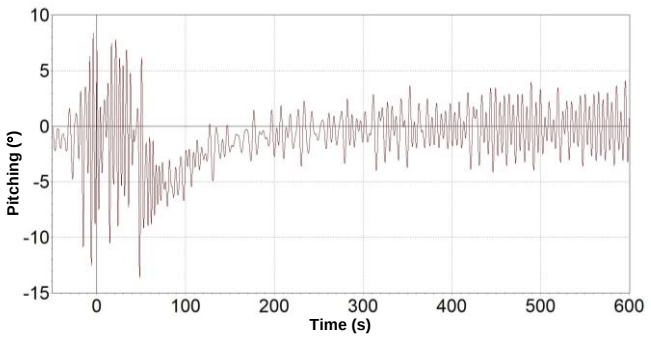

(a) T = 9 sec

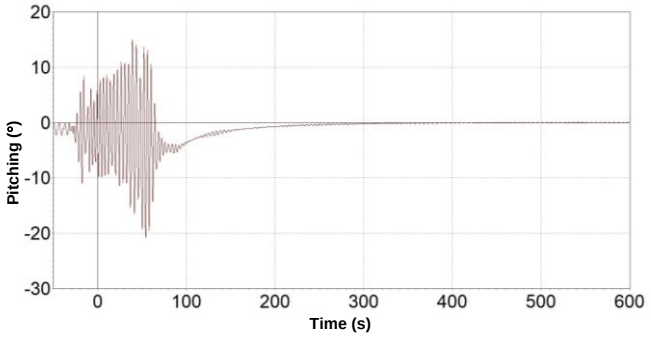

(b) T = 3 sec

Fig. 14 System pitch motion for the wire rope with d = 3 cm.

VI. Conclusions

In the present study, we have investigated the effect of mooring line type on the FKT system dynamics. Three different types of mooring line were studied. They are the polyester rope, the iron chain, and the wire rope.

Without wave impact, the polyester rope could lead to system fluctuation or instability if its diameter is not big enough. The system performance due to the iron chain and wire rope is much better improved. In fact, the system fluctuation in deployment could be related to the linear mass density of mooring line. If the linear mass density is more than some critical value, the system can exhibit good stability in normal operation conditions.

With wave impact, we found that the iron chain could have better performance than the wire rope in the sense that the system fluctuation is much smaller in a normal operation condition. In summary, the iron chain is a better choice within the three types of mooring line for the present floating Kuroshio turbine system with a Y-shape mooring line system.

Acknowledgment

The study was made possible with the grant from Ministry of Science and Technology, the Republic of China, under the contract MOST 105-3113-E-002-019-CC2 and funding support from CSBC Corporation.

References

[1] J. Van Zwieten, F.R. Driscoll, A. Leonessa, and G. Deane, "Design of a prototype ocean current turbine---Part I: mathematical modeling and dynamics simulation," *Ocean Eng.*, Vol. 33, pp. 1485-1521, 2006.

[2] F. Chen, *The Kuroshio Power Plant*, Switzerland: Springer, 2013.

[3] IHI Corporation, "Power generation using the Kuroshio Current," *IHI Eng. Review*, Vol. 46, pp. 2-5, 2014.
[4] J.-Y. Bai, "Ocean current power generation project," *Workshop on Development of Marine Mechanical Energy Industry in Taiwan*, Keelung, Taiwan, 2012 (in Chinese).
[5] A. Røkke and R. Nilssen, "Marine current turbines and generator preference: A technology review," *Int. Conf. Renew. Energies Power Quality*, Bilbao, Spain, 2013.
[6] Y. Kyozuka, "Tidal and ocean current power generation," *J. Smart Processing*, Vol. 3, pp. 137-145, 2014.
[7] A.R. Cribbs, "Model analysis of a mooring system for an ocean current turbine testing platform," M.S. thesis, Florida Atlantic University, Boca Raton, Florida, USA, Dec. 2010.
[8] A.R. Cribbs and J.H. VanZwieten, "Global numerical analysis of a moored ocean current turbine testing platform," *Oceans*, Seattle, OR, USA, 2010.
[9] M. Shibata, K. Takeda, and K. Takgai, "Mooring and power cable system for current-turbine," *Oceans*,San Diego, CA, USA, 2013.
[10] K. Takagi, T. Waseda, S. Nagaya, Y. Niizeki, and Y. Oda, "Development of a floating current turbine," *Oceans*, Hampton Roads, VA, USA, 2012.
[11] Y.-H. Rho, C.-H. Jo, and D.-Y. Kim, "Optimization of mooring system for multi-arrayed tidal turbines in a strong current area," *Proc. ASME 33rd Int. Conf. Ocean, Offshore and Arctic Eng.*, San Francisco, CA, USA, 2014.
[12] C.C. Tsao and A.H. Feng, "Motion Model and Speed Control of the Cross-Stream Active Mooring System for Tracking Short-Term Meandering to Maximize Ocean Current Power Generation," *J. Mech.*, 1-15, 2017.
[13] K. Shirasawa, J. Minami, and T. Shintake, "Scale-model experiments for the surface wave influence on a submerged floating ocean-current turbine," *Energies*, Vol. 10, 702, 2017.
[14] J.-T. Wu, J.-H. Chen, C.-Y. Hsin, and F.-C. Chiu, "A computational study on system dynamics of an ocean current turbine," *J. Hydrodyn.*, accepted, 2018.
[15] A.R. Cribbs, G.R. Karrsten, J.T. Shelton, R.S. Nicoll, and W.P. Stewart, "Mooring system considerations for renewable energy standards," *Offshore Technology Conf.*, Houston, TX, USA, 2017.
[16] A.E.D. Bowie, "Flexible moorings for tidal current turbines," M.S. thesis, University of Strathclyde, Glasgow, UK, Sep. 2012.
[17] C.H. Jo, D.Y. Kim, B.K. Cho, and M.J. Kim, "Mooring analysis of duct-type tidal current power system in shallow water," *Int. J. Geol. Environ. Eng.*,Vol. 10, pp. 577-582, 2016.
[18] D.W. Atkins, "The CFD assisted design and experimental testing of a wingsail with high lift devices," Ph.D. dissertation, University of Salford, Salford, UK, 1996.
[19] H.Y. Lo, "Dynamic analysis of current turbine system," M.S. thesis, National Taiwan Ocean University, Keelung, Taiwan, 2017 (in Chinese).